



# Direct electrolysis of CO<sub>2</sub> using an oxygen-ion conducting solid oxide electrolyzer based on La<sub>0.75</sub>Sr<sub>0.25</sub>Cr<sub>0.5</sub>Mn<sub>0.5</sub>O<sub>3-δ</sub> electrode

Shanshan Xu<sup>a</sup>, Shisong Li<sup>a</sup>, Weitang Yao<sup>a</sup>, Dehua Dong<sup>b</sup>, Kui Xie<sup>a,\*</sup>

<sup>a</sup> Department of Energy Materials, School of Materials Science and Engineering, Hefei University of Technology, No.193 Tunxi Road, Hefei, Anhui 230009, China

<sup>b</sup> Fuels and Energy Technology Institute, Curtin University of Technology, 1 Turner Avenue, Technology Park, WA 6102, GPO Box U1987, Perth, WA 6845, Australia

## HIGHLIGHTS

- Electrolysis of CO<sub>2</sub> is demonstrated in a symmetric cell with LSCM electrode.
- LSCM electrode shows excellent performance with current for activation in air.
- LSCM electrode markedly improves with current for activation in CO<sub>2</sub>.
- Reduction of LSCM is the main process at low voltage during electrolysis.
- Electrochemical reduction of CO<sub>2</sub> is main process at high voltage in electrolysis.

## ARTICLE INFO

### Article history:

Received 14 September 2012

Received in revised form

15 November 2012

Accepted 17 December 2012

Available online 27 December 2012

### Keywords:

Electrolysis

Carbon dioxide

Oxygen-ion conductor

La<sub>0.75</sub>Sr<sub>0.25</sub>Cr<sub>0.5</sub>Mn<sub>0.5</sub>O<sub>3-δ</sub>

Solid oxide electrolyzer

## ABSTRACT

Composite fuel electrode based on redox-reversible La<sub>0.75</sub>Sr<sub>0.25</sub>Cr<sub>0.5</sub>Mn<sub>0.5</sub>O<sub>3-δ</sub> (LSCM) can be operated without a flow of reducing gas. We demonstrate the efficient electrolysis of CO<sub>2</sub> using a symmetric solid oxide electrolyzer with a configuration of LSCM–SDC/YSZ/LSCM–SDC at 800 °C. The temperature dependence of LSCM conductivity in air and the oxygen partial pressure dependence are investigated and correlated to electrode polarization in the symmetric cell. The LSCM electrode exhibits low electrode polarization in air at 800 °C (0.325 Ω cm<sup>2</sup>), and the electrode polarization can be further reduced to 0.25 Ω cm<sup>2</sup> when passing current to activate LSCM electrodes. In contrast, the electrode polarization of the symmetric cell in CO<sub>2</sub> reached 5–10 Ω cm<sup>2</sup> under OCV and low current. However, it is decreased to 0.5 Ω cm<sup>2</sup> at large currents (e.g. 100–200 mA cm<sup>-2</sup>) for electrode activation. The results of AC impedance spectroscopy and *I*–*V* tests indicate two main processes: the electrochemical reduction of LSCM fuel electrode at low voltages and the electrolysis of CO<sub>2</sub> at high voltages. The current efficiency reaches 69%, 58% and 56% at 1.0, 1.5 and 2.0 V for the electrolysis of CO<sub>2</sub> at 800 °C, respectively.

© 2012 Elsevier B.V. All rights reserved.

## 1. Introduction

Solid oxide electrolyzer (SOE) is the inverse running of solid oxide fuel cells (SOFC). It is a promising electrochemical device that converts electrical energy into chemical energy directly [1–3]. In recent years, SOE has been attracting a great deal of interests. High temperature SOE is operated at temperatures ranging from 700 °C to 1000 °C without using expensive noble metals as electrodes [4,5]. The solid state device has a long lifetime through avoiding the corrosion and evaporation caused by liquid electrolytes [5]. High-temperature electrolysis process is promising because the heat partly offers the energy for molecular dissociation and then leads to favorable kinetics and thermodynamics [4].

At present, the massive carbon dioxide emission leads to the serious global warming and climate change [6]. High-temperature electrolysis exhibits great promise in the electrolysis of CO<sub>2</sub> using a SOE [1,7–10]. Applying external potential, an oxygen-ion conducting solid oxide electrolyzer is able to electrolyze carbon dioxide into carbon monoxide and oxygen. On the fuel electrode side, CO<sub>2</sub> molecules are electrochemically reduced into CO. The oxygen ions are transported through the oxygen-ion conducting electrolyte to the oxygen electrode compartment where O<sub>2</sub> gas is formed and released [4,11]. Currently, most reports of high temperature electrolysis of CO<sub>2</sub> have been preferentially performed with Ni–YSZ composite fuel electrode in SOEs [12,13]. However, a significant concentration of CO is required to flow over Ni cermet to avoid the oxidation of Ni to NiO, which would cause a loss of electronic conductivity and the failure of electrode. In addition, the poor resistance to redox cycling, causing and low long-term morphology and performance stability prevents its

\* Corresponding author. Tel./fax: +86 551 2905413.

E-mail address: [xiekui@hfut.edu.cn](mailto:xiekui@hfut.edu.cn) (K. Xie).

application in SOE [14–16]. It has been found that the perovskite ceramic  $\text{La}_{0.75}\text{Sr}_{0.25}\text{Cr}_{0.5}\text{Mn}_{0.5}\text{O}_{3-\delta}$  (LSCM) is an efficient anode material for SOFC, which exhibits comparable anode performances to the traditional Ni–YSZ cermet [17–19]. The perovskite LSCM is an active and redox-stable material, and has attracted extensive attention as the high-temperature SOFC anode [20–22]. Especially, LSCM can be used for both anode and cathode [23,24]. In other words, LSCM electrode can work under extreme oxidizing or reducing atmospheres.

In our work, we aim to directly perform the electrolysis of  $\text{CO}_2$  in a symmetric cell with a configuration of LSCM–SDC/YSZ/LSCM–SDC, which avoids the use of a flow of reducing gas like CO to protect the fuel electrode from being oxidized. The electrical prosperities of LSCM are studied and correlated to the electrode performances in the symmetric cell under different operating conditions. Direct electrolysis of  $\text{CO}_2$  in the as-prepared symmetric SOE is evaluated and discussed in this paper.

## 2. Experimental

The perovskite  $\text{La}_{0.75}\text{Sr}_{0.25}\text{Mn}_{0.5}\text{Cr}_{0.5}\text{O}_{3-\delta}$  (LSCM) powders are prepared by a combustion method using  $\text{La}_2\text{O}_3$ ,  $\text{Sr}(\text{NO}_3)_2$ ,  $\text{Cr}(\text{NO}_3)_3 \cdot 9\text{H}_2\text{O}$  and  $\text{C}_4\text{H}_6\text{MnO}_4 \cdot 4\text{H}_2\text{O}$  followed by a heat treatment at  $1200^\circ\text{C}$  for 5 h in air [22,25]. The  $\text{Ce}_{0.8}\text{Sm}_{0.2}\text{O}_{2-\delta}$  (SDC) powders are prepared from  $\text{Sm}_2\text{O}_3$  and  $\text{Ce}(\text{NO}_3)_4 \cdot 6\text{H}_2\text{O}$  using the same method. The final heat treatment is conducted at  $800^\circ\text{C}$  for 2 h in air. All these chemicals (Chemical grade) are purchased from SINOPHARM

Chemical Reagent Co., Ltd (China). The X-ray diffraction (XRD,  $2\theta = 3^\circ \text{ min}^{-1}$ , D/MAX2500V, Rigaku Corporation, Japan) is performed to analyze the phase purity of the LSCM and SDC powders. A proper amount of LSCM powder was pressed into a bar, followed by sintering at  $1400^\circ\text{C}$  for 10 h in air for conductivity test. The sample relative density reached 83%. Conductivity test of LSCM was carried out in air using dc four-terminal method from room temperature to  $800^\circ\text{C}$ , and the conductivity was recorded with an online system at a step of  $0.4^\circ\text{C}$ . The partial oxygen pressure dependence of conductivity was tested at  $800^\circ\text{C}$  with oxygen partial pressures ranging from 0.2 to  $10^{-20}$  atm. 5% $\text{H}_2/\text{Ar}$  was initially input at the flow rate of  $20 \text{ ml min}^{-1}$  to control the  $\text{Po}_2$  at  $10^{-20}$  atm. Then air was supplied at the flow rate of  $0.5 \text{ ml min}^{-1}$  to increase the oxygen partial pressure after the stop of flow of 5% $\text{H}_2/\text{Ar}$ . The oxygen partial pressure ( $\text{Po}_2$ ) and conductivity were recorded with an online oxygen sensor (Type 1231,  $\text{ZrO}_2$ -based oxygen sensor, Noveltech, Australia) and an online multimeter (Keithley 2000, Digital Multimeter, Keithley Instruments, Inc., USA) while the total gas pressure was controlled at 1.0 atm.

A 2-mm-thick 8YSZ disc electrolyte support was prepared by dry-pressing the 8YSZ powder into a green disk with a diameter of 20 mm, and then the disk was sintered in air at  $1450^\circ\text{C}$  ( $3^\circ\text{C min}^{-1}$ ) for 10 h. The two surfaces of the obtained YSZ electrolyte support were mechanically polished and then washed by ethanol and distilled water in an ultrasonic cleaner. The composite electrode LSCM–SDC slurry was prepared by grinding the mixture of SDC powder and the LSCM powder at a weight ratio of 40:60 with the

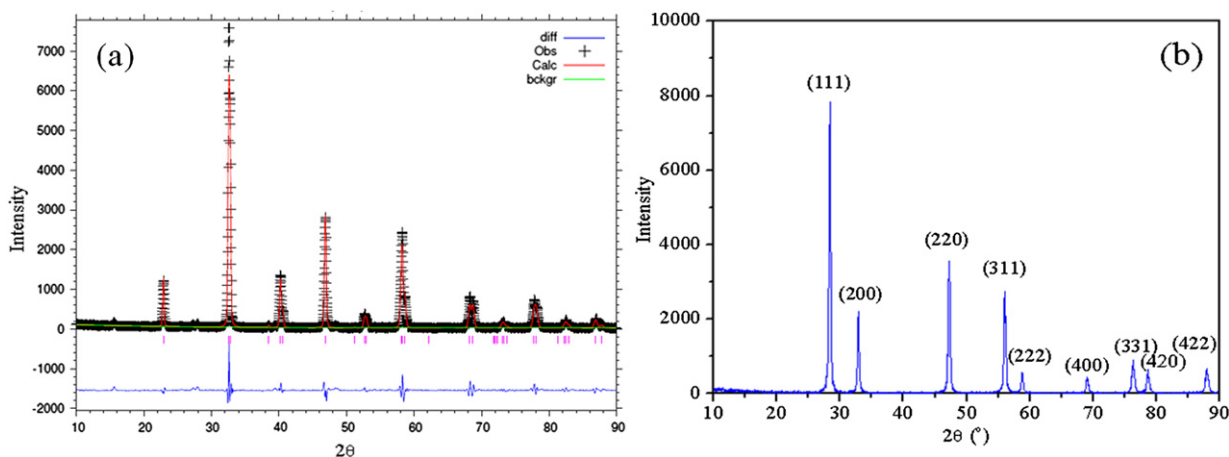


Fig. 1. XRD Retiveld refinement of the (a)  $\text{La}_{0.75}\text{Sr}_{0.25}\text{Cr}_{0.5}\text{Mn}_{0.5}\text{O}_{3-\delta}$  (LSCM) and (b)  $\text{Ce}_{0.8}\text{Sm}_{0.2}\text{O}_{2-\delta}$  (SDC) ceramic powders.

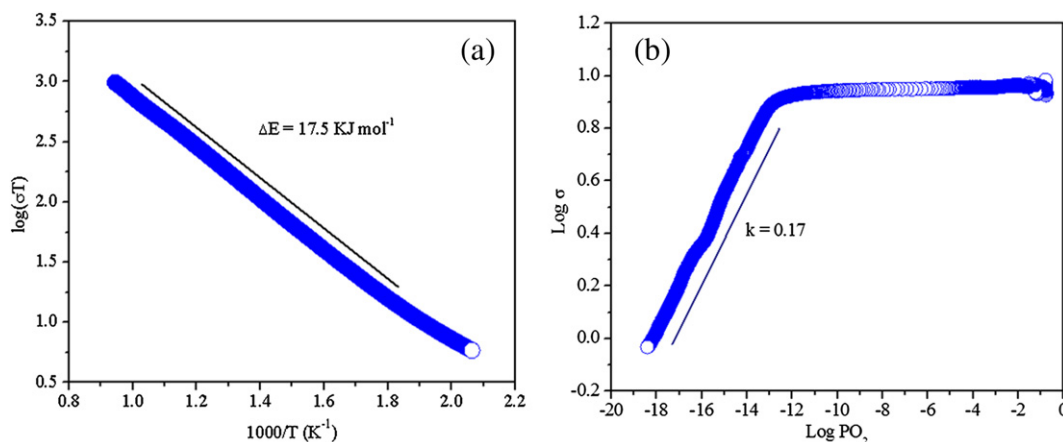
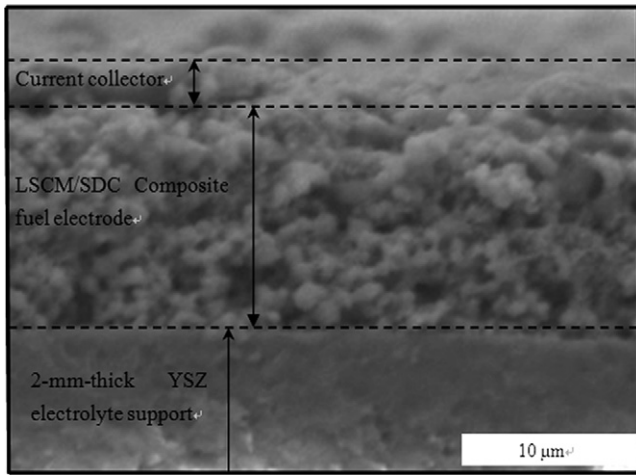


Fig. 2. The conductivity of LSCM affected by (a) temperature from room temperature to  $800^\circ\text{C}$  in air and (b) oxygen partial pressure ranging from  $10^{-1}$  to  $10^{-20}$  atm at  $800^\circ\text{C}$ .



**Fig. 3.** The SEM image of the symmetric solid oxide electrolyzer with a configuration of LSCM–SDC/YSZ/LSCM–SDC.

addition of alpha-terpineol and cellulose. The two electrodes were then coated onto the both sides of YSZ electrolyte in symmetric positions with an area of  $1 \text{ cm}^2$ , followed by a heat treatment at  $1100^\circ\text{C}$  ( $3^\circ\text{C min}^{-1}$ ) for 3 h in air. The current collection layer was made by painting silver paste (SS-8060, Xinluyi, Shanghai, China)

on electrode surfaces. The microstructure of the as-prepared electrolyzer was observed with a scanning electron microscope (SEM, JSM-6490LV, JEOL Ltd, Japan). The external circuit was made with silver electrical wire (0.1 mm in diameter), which was then connected to both current collectors using silver paste (DAD87, Shanghai Research Institute for Synthetic Resins), followed by firing at  $550^\circ\text{C}$  for 30 min in air. The single solid oxide electrolyzer was sealed to a home-made testing jig using ceramic paste (JD-767, Jiudian, Dongguan, China) for electrochemical measurements. AC impedance of the symmetric SOE was tested with static air on oxygen electrode side and  $\text{CO}_2$  on fuel electrode side, applying different currents passing through the symmetric cell for electrode activation at  $800^\circ\text{C}$  using an electrochemical station (IM6, Zahner, Germany). The gas flow rate was controlled at  $40 \text{ ml min}^{-1}$  using mass flow meter (D08-3F, Sevenstar, Beijing, China). Electrochemical measurements including AC impedance and current–voltage ( $I$ – $V$ ) curves of the SOE were performed (two-electrode type) with the two electrodes exposed to flowing  $\text{CO}_2$  and static air at  $800^\circ\text{C}$ . The direct electrolysis of  $\text{CO}_2$  was performed at the external potentials of 0.5, 1.0, 1.5 and 2.0 V at  $800^\circ\text{C}$ , respectively. The exit gas from the fuel electrode was analyzed using an online gas chromatograph (GC9790II, Fuli, Zhejiang, China), the concentration of carbon monoxide was calculated. Synchrotron radiation XRD ( $K\alpha=1.40 \text{ \AA}$ , Shanghai Light Source, Shanghai, China) was conducted to analyze the LSCM powder before and after the treatment in  $5\%\text{H}_2/\text{Ar}$  at  $800^\circ\text{C}$  for 2 h.

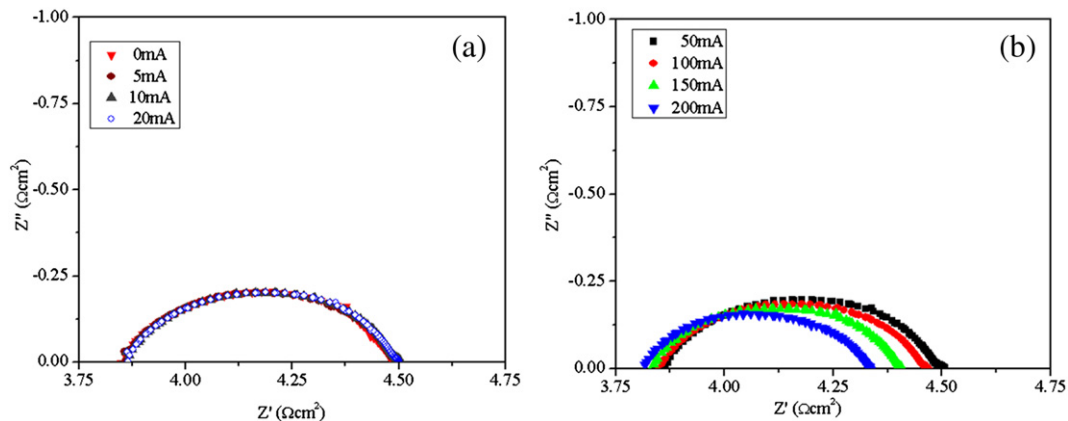


**Fig. 4.** AC impedance spectra of the symmetric SOE with the configuration of LSCM–SDC/YSZ/LSCM–SDC tested at  $800^\circ\text{C}$  with two electrodes exposed to air.

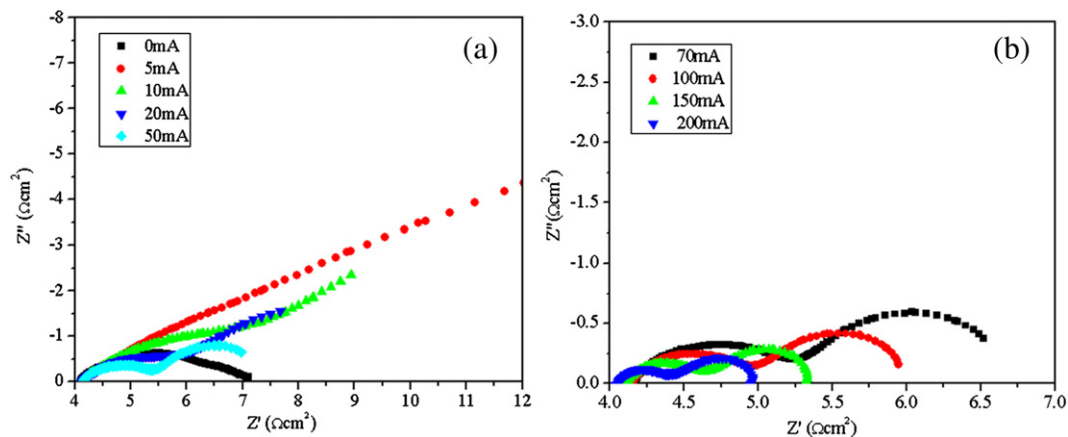


**Fig. 5.** AC impedance spectra of the symmetric SOE with configuration of LSCM–SDC/YSZ/LSCM–SDC tested at  $800^\circ\text{C}$  with two electrodes exposed to  $\text{CO}_2$  and under different applying current densities.

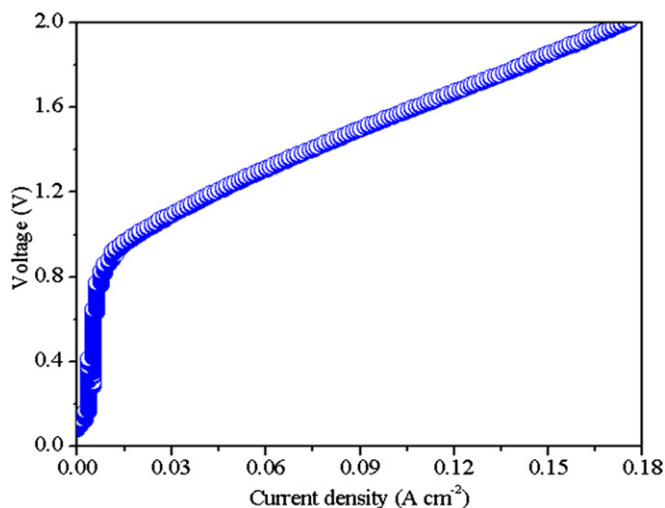


Fig. 6.  $I$ – $V$  curve of the symmetric SOE with configuration of LSCM–SDC/YSZ/LSCM–SDC tested at 800 °C with  $\text{CO}_2$  fed into fuel electrode and oxygen electrode exposed in air.

### 3. Results and discussions

Fig. 1 shows the XRD patterns of SDC and LSCM powders after a heat treatment at 800 °C and 1200 °C in air, respectively, which indicate that both SDC and LSCM are in pure phases [21,26]. Fig. 1(a) shows the XRD Rietveld refinement of as-prepared LSCM sample, which has the strong peaks corresponding to space group R-3c ( $a = 0.549833$  nm;  $b = 0.549833$  nm;  $c = 1.33449$  nm;  $\alpha = 90^\circ$ ;  $\beta = 90^\circ$ ;  $\gamma = 120^\circ$ ). The refinement of LSCM sample gives  $\chi^2$ ,  $wRp$  and  $R_p$  values of 3.432, 0.1553 and 0.1117, respectively, indicating a good fit to the experimental data. Fig. 1(b) shows the XRD pattern of SDC powder as well as the crystal indices of peaks, indicating a pure cubic phase. The LSCM is a p-type electronic conductor. As shown in Fig. 2(a), the temperature dependence of conductivity shows a typical semiconducting behavior having a positive coefficient with temperature up to 800 °C in air. The conductivity of the LSCM reaches approximately  $10 \text{ S cm}^{-1}$  at 800 °C with the activation energy ( $\Delta E$ ) of  $17.5 \text{ kJ mol}^{-1}$ . The p-type conducting properties are also observed, as shown in Fig. 2(b). The conductivity of the LSCM sample is independent on the oxygen partial pressure at 800 °C when oxygen partial pressure is above  $10^{-14}$  atm. However, the conductivity significantly decreases when the oxygen partial pressure is below  $10^{-14}$  atm. The conductivity

decreases to  $0.5 \text{ S cm}^{-1}$  at 800 °C, which is probably attributed to the decrease of the charge carrier concentration. The oxygen partial pressure greatly influences the conductivity of LSCM ceramic, which might be presented in the form of electrode polarization during the electrolysis of  $\text{CO}_2$  in the SOE.

Fig. 3 shows the SEM image of the symmetric electrolyte-supported SOE before test. It is observed that a single SOE is constructed on YSZ electrolyte support with two composite LSCM/SDC electrodes. The two porous electrodes layers with the thickness of 10  $\mu\text{m}$  adhere to the electrolyte by sintering. The porous silver current collector layer is around 2  $\mu\text{m}$  in thickness. Fig. 4(a) and (b) show the AC impedance of the symmetric LSCM–SDC/YSZ/LSCM–SDC SOE at 800 °C with two electrodes exposed to static air under different current densities. The intercept of the impedance spectra with the real axis at the high frequency corresponds to the ohmic resistance ( $R_s$ ) of the cell, which mainly results from the ionic transfer resistance of YSZ electrolyte. The ohmic resistance is about  $3.88 \Omega \text{ cm}^2$  at low current density while a slight decrease is observed at high current densities, which is probably due to the p-type conduction in YSZ electrolyte. On the other hand, the variation of  $R_s$  might also be related to the changes in the electrode polarizations ( $R_p$  element) affecting the intercept, particularly at lower  $R_p$  values, enhancement of lateral conductivity in oxygen electrode at high potentials. As shown in Fig. 4(a), the polarization resistance ( $R_p$ ) is approximately  $0.325 \Omega \text{ cm}^2$  at low current densities. However, the electrode polarization is further reduced to  $0.25 \Omega \text{ cm}^2$  at high current densities for electrode activation. Fig. 5(a) and (b) shows AC impedance of the symmetric cell LSCM–SDC/YSZ/LSCM–SDC at 800 °C with two electrodes exposed to pure  $\text{CO}_2$  under different current densities passing through the cell. Similarly, only slight change of  $R_s$  is observed while the electrode polarization of the symmetric cell,  $R_p$ , in  $\text{CO}_2$  significantly changes with current density. The electrode polarization resistance is about  $1.5 \Omega \text{ cm}^2$  without current passing the cell while it reaches 5–10  $\Omega \text{ cm}^2$  at low current densities, which is probably attributed to the significant decrease of LSCM conductivity in pure  $\text{CO}_2$  compared to that in air. It should be noted that the  $R_p$  is significantly decreased at larger current densities for electrodes activation. The  $R_p$  reaches  $0.5 \Omega \text{ cm}^2$  under the current density of  $200 \text{ mA cm}^{-2}$ . It is therefore to speculate that the electrode polarization resistance of the symmetric SOE is mainly contributed by the fuel electrode when the electrolysis of  $\text{CO}_2$  is performed.

Fig. 6 shows the typical voltage versus current density ( $I$ – $V$ ) curve of the symmetric cell LSCM–SDC/YSZ/LSCM–SDC at 800 °C with  $\text{CO}_2$  fed into fuel electrode and oxygen electrode exposed to air. The open circuit voltage (OCV) of the electrolyzer is approximately

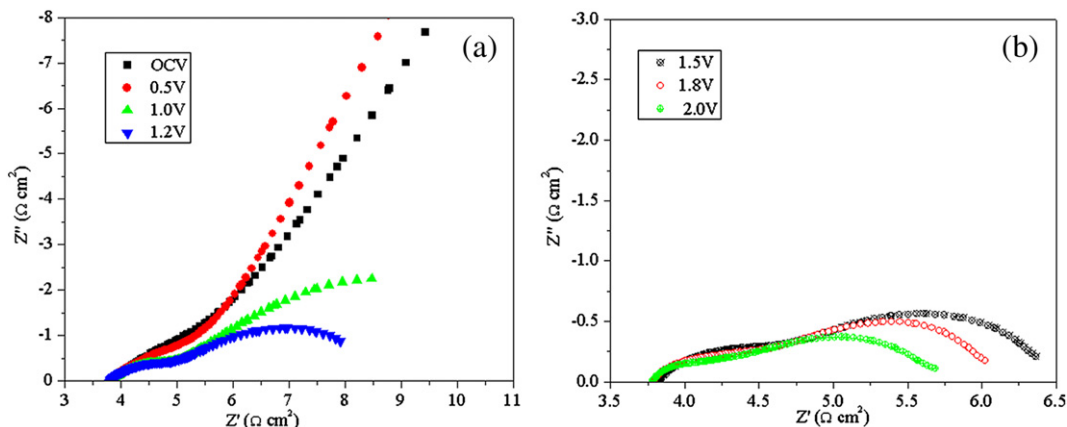


Fig. 7. AC impedance spectra of the symmetric SOE with the configuration of LSCM–SDC/YSZ/LSCM–SDC at 800 °C and different applied voltages.



0.38 V, which is consistent with  $\text{CO}_2/\text{O}_2$  concentration cell (0.1–0.6 V) [27]. However, it should be noted that the OCV observed from the  $I$ – $V$  curves is much low, which might be due to that the cell is not at a proper equilibrium state during the test. The relationship between current and voltage is far from linear, with a remarkable increase as current increases. The maximum current density reaches  $0.18 \text{ A cm}^{-2}$  at 2 V, which is about 1 V above the open circuit potential of the  $\text{CO}/\text{air}$  system. In order to study the change of cell resistance under different voltages, in-situ AC impedance spectroscopy is therefore carried out under different loads to investigate the  $R_s$  and  $R_p$  changes, where the  $R_s$  and  $R_p$  correspond to the series resistance and electrode polarizations of cell, respectively.

Fig. 7 shows the AC impedance spectra of the symmetric cell at  $800^\circ\text{C}$  and different applied voltages.  $R_s$  is about  $3.8 \Omega \text{ cm}^2$ , which is consistent with the ionic resistance of the YSZ disk at  $800^\circ\text{C}$ . The electrode polarization resistance,  $R_p$ , is considerably large, reaching  $10$ – $20 \Omega \text{ cm}^2$  under the open circuit condition and at low voltages. According to the results discussed above in Fig. 5, it is reasonable to speculate that the electrode polarization of the fuel electrode in pure  $\text{CO}_2$  dominates the total cell performance at low voltages. However, the increased voltage significantly activates the LSCM/SDC fuel electrode and makes the  $R_p$  decrease to  $2.0 \Omega \text{ cm}^2$  at 2.0 V. At this stage, the  $R_s$  dominates the total cell performance at high voltage because it is 2/3 of the total cell resistance. Accordingly, the ionic transport in YSZ electrolyte is the limiting step. There are two main regions from 0 to 2 V in the electrolysis process of  $\text{CO}_2$  at  $800^\circ\text{C}$ . The electrochemical reduction of LSCM fuel electrode is the main process below 1.0 V, while the electrolysis of  $\text{CO}_2$  should be the controlling step above 1.0 V.

Fig. 8 shows the short-term performance of the symmetric cell for the electrolysis of  $\text{CO}_2$  at  $800^\circ\text{C}$  and at different applied voltages. The current densities are recorded as function of time at the applied voltages of 0.5, 1.0, 1.5 and 2.0 V for the electrolysis of  $\text{CO}_2$ , respectively. The current density reaches  $0.005 \text{ A cm}^{-2}$  at the applied voltage of 0.5 V. However, the electrolysis of  $\text{CO}_2$  should not start because the OCV of  $\text{CO}$ -fueled SOFC is approximately 0.9 V [28,29], which is further confirmed by the absence of  $\text{CO}$  production at 0.5 V, as shown in Fig. 9. At the voltage of 1.0 V, the electrochemical reduction of  $\text{CO}_2$  starts and produces  $\text{CO}$  with the rate of  $0.03 \text{ ml min}^{-1} \text{ cm}^{-2}$  at current density  $0.01 \text{ A cm}^{-2}$ . The significant increases of current density (0.09 and  $0.18 \text{ A cm}^{-2}$ ) are observed when the applied voltages increase to 1.5 and 2.0 V,

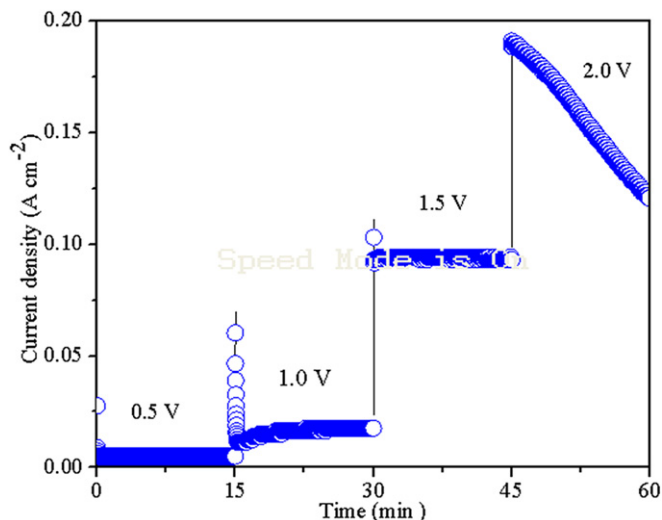


Fig. 8. Performance of the symmetric SOE with the configuration of LSCM–SDC/YSZ/LSCM–SDC for electrolysis of  $\text{CO}_2$  at  $800^\circ\text{C}$  at different applied voltages.

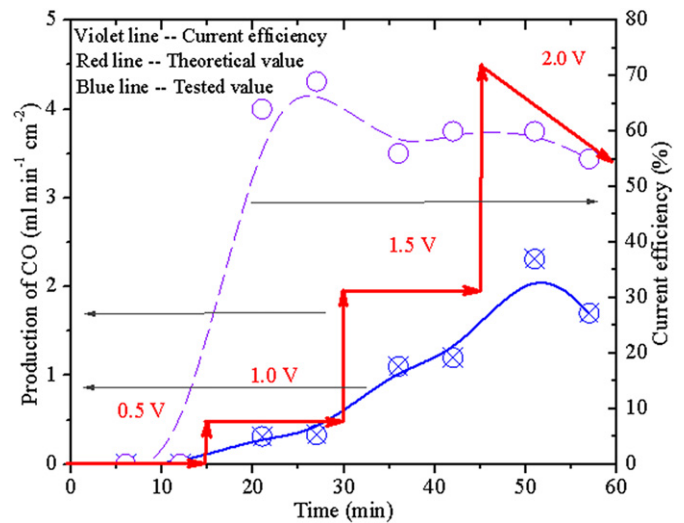


Fig. 9. Production of carbon monoxide and current efficiency from the electrolysis of  $\text{CO}_2$  in the symmetric SOE with the configuration of LSCM–SDC/YSZ/LSCM–SDC at  $800^\circ\text{C}$  and different applied voltages.

respectively, which is possibly due to the effective activation of LSCM electrode. Furthermore, the favorable kinetics and thermodynamics at high voltages would lead to efficient electrode process, which might be able to improve the electrode polarization. The  $\text{CO}$  is accordingly increased to 1.2 and  $2.0 \text{ ml min}^{-1} \text{ cm}^{-2}$ , respectively. The current efficiency at 1.0 V reaches 69%, which is higher than that for 1.5 V (58%) and 2.0 V (56%). This is probably due to the local starvation of  $\text{CO}_2$  at high voltages for the electrochemical reduction because the adsorption of  $\text{CO}_2$  in fuel electrode could be a limiting step. However, it should be noted that the current density at the applied voltage of 2.0 V rapidly degrades with time, which could be due to the chemical changes of LSCM electrode at strong reducing potential of 2.0 V. It has been reported that LSCM could be reduced into a cubic structure in 5% $\text{H}_2/\text{Ar}$  at  $900^\circ\text{C}$ , which may be presented at 2.0 V and  $800^\circ\text{C}$  in this experiment [30,31].

In order to further check the performance of the solid oxide cell, another short-term performance test is performed with two electrodes exposed to static air and pure  $\text{CO}_2$ , respectively. However, different voltages are applied for the electrolysis of  $\text{CO}_2$  at  $800^\circ\text{C}$  and the current densities are recorded as a function of time. As

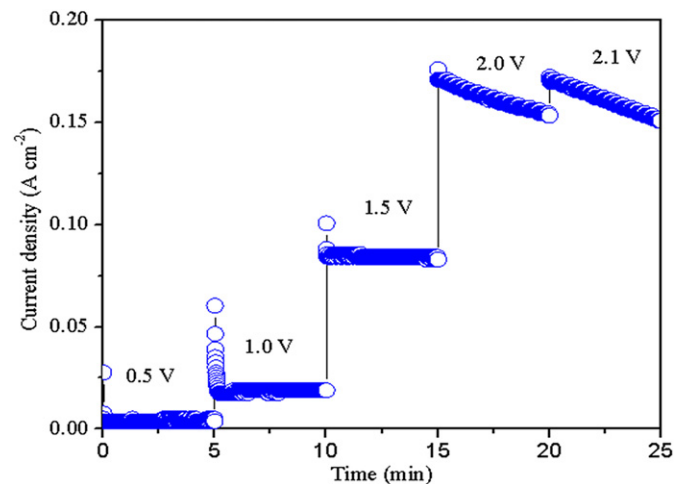


Fig. 10. Performance of the symmetric SOE with the configuration of LSCM–SDC/YSZ/LSCM–SDC for the electrolysis of  $\text{CO}_2$  at  $800^\circ\text{C}$  repeatedly tested at different applied voltages.

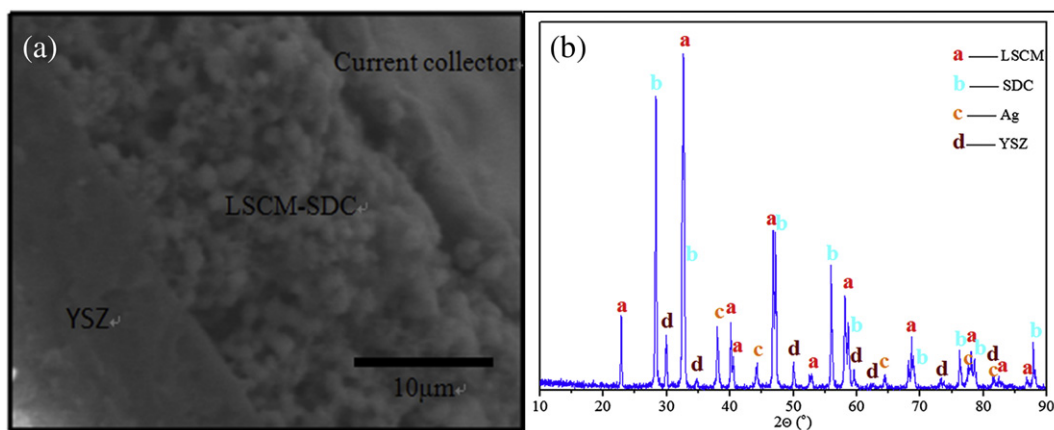


Fig. 11. The SEM image (a) and XRD (b) of the LSCM–SDC fuel electrode after the test of the electrolysis of CO<sub>2</sub>.

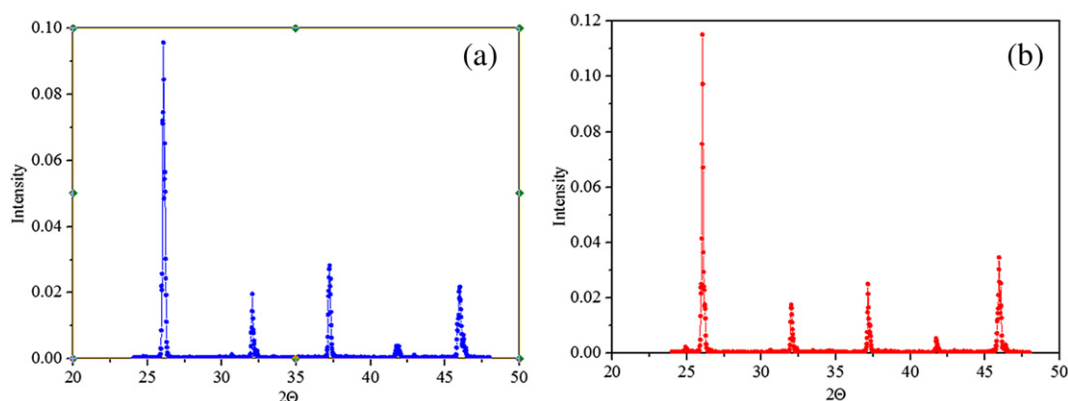


Fig. 12. Synchrotron radiation XRD ( $K\alpha=1.40 \text{ \AA}$ ) of the  $\text{La}_{0.75}\text{Sr}_{0.25}\text{Cr}_{0.5}\text{Mn}_{0.5}\text{O}_{3-\delta}$  (LSCM) powder before (a) and after (b) the treatment in 5%  $\text{H}_2/\text{Ar}$  at 800 °C for 2 h.

shown in Fig. 10, the similar behavior of the cell is observed at low voltages as discussed above. However, the current density still degrades at the voltages of 2.0 V and 2.1 V, which confirms that the phenomenon is completely reversible. As shown in Fig. 11(a), no microstructure change is observed in electrodes, which indicates that the electrodes based on LSCM did not change or detach from the YSZ electrolyte. In other words, the degradation of cell performance might be caused by the chemical change of LSCM. XRD is employed to analyze the fuel electrode side of the cell after test, as shown in Fig. 11(b). It is observed that the fuel electrode is composed of LSCM, SDC, YSZ and Ag. More importantly, the LSCM electrode material has no crystal structure change according to the XRD, which indicates that the change of LSCM might be reversible. To further confirm the reversible change of LSCM, synchrotron radiation XRD is utilized to characterize the LSCM powder before and after the treatment in 5%  $\text{H}_2/\text{Ar}$  at 800 °C for 2 h. As shown in Fig. 12(a) and (b), the crystal structure of LSCM ceramic is not changed after the treatment in 5%  $\text{H}_2/\text{Ar}$  at 800 °C, indicating a good redox-reversible property. To further confirm the chemical change of LSCM under strongly reducing potential in electrolyzer, in-situ synchrotron radiation XRD is to be utilized in our future work because ex-situ XRD is not able to confirm the chemical change of LSCM.

#### 4. Conclusion

In this work, a composite electrode based on  $\text{La}_{0.75}\text{Sr}_{0.25}\text{Cr}_{0.5}\text{Mn}_{0.5}\text{O}_{3-\delta}$  (LSCM) is investigated in an oxygen-ion conducting solid oxide electrolyzer with a configuration of LSCM–SDC/YSZ/LSCM–SDC at 800 °C. The electrical properties of LSCM is

investigated and correlated to the electrode polarizations in the symmetric cell. The LSCM electrode in symmetric cell exhibits high performance in CO<sub>2</sub> when applying large current densities for electrode activation at 800 °C. The direct electrolysis of CO<sub>2</sub> is performed in this cell under different applied voltages at 800 °C. The results of AC impedance spectroscopy and  $I$ – $V$  tests indicate two main processes from 0 to 2 V with CO<sub>2</sub>/air system: the reduction of the LSCM electrode below 1.0 V and the electrolysis of CO<sub>2</sub> above 1.0 V. The current efficiency reaches approximately 69%, 58% and 56% at 1.0, 1.5 and 2.0 V for the electrolysis of CO<sub>2</sub> at 800 °C, respectively. It is supposed that the chemical change of LSCM electrode occurs under the strong reducing potential of 2.0 V that leads to the degradation of cell performance at high voltages. However, it is also observed that the degradation of cell performance can be recovered in the repeated experiment.

#### Acknowledgment

The authors would like to thank the support of NSFC Nos. 51142008.

#### References

- [1] F. Bidrawn, G. Kim, G. Corre, J.T.S. Irvine, J.M. Vohs, R.J. Gorte, *Electrochem. Solid State Lett.* 11 (2008) B167–B170.
- [2] T. Ishihara, N. Jirathiwathanakul, H. Zhong, *Energy Environ. Sci.* 3 (2010) 665.
- [3] G. Tsekouras, J.T.S. Irvine, *J. Mater. Chem.* 21 (2011) 9367.
- [4] A. Hauch, S.D. Ebbesen, S.H. Jensen, M. Mogensen, *J. Mater. Chem.* 18 (2008) 2331.
- [5] X.D. Yang, J.T.S. Irvine, *J. Mater. Chem.* 18 (2008) 2349.
- [6] K. Xie, Y.Q. Zhang, G.Y. Meng, J.T.S. Irvine, *Energy Environ. Sci.* 4 (2011) 2218.

- [7] K. Xie, Y.Q. Zhang, G.Y. Meng, J.T.S. Irvine, *J. Mater. Chem.* 21 (2011) 195.
- [8] G. Ta, K.R. Sridhar, C.L. Chan, *Solid State Ionics* 175 (2004) 615.
- [9] C. Graves, S.D. Ebbesen, M. Mogensen, *Solid State Ionics* 192 (2011) 398.
- [10] X. Yue, J.T.S. Irvine, *Electrochem. Solid State Lett.* 15 (2012) B31–B34.
- [11] S.S. Li, Y.X. Li, Y. Gan, K. Xie, G.Y. Meng, *J. Power Sources* 218 (2012) 244.
- [12] S.D. Ebbesen, R. Knibbe, M. Mogensen, *J. Electrochem. Soc.* 159 (2012) F482–F489.
- [13] S.D. Ebbesen, M. Mogensen, *J. Power Sources* 193 (2009) 349.
- [14] S.W. Tao, J.T.S. Irvine, *Chem. Mater.* 16 (2004) 4116.
- [15] E.S. Raj, J.A. Kilner, J.T.S. Irvine, *Solid State Ionics* 177 (2006) 1747.
- [16] S.W. Tao, J.T.S. Irvine, *Chem. Rec.* 4 (2004) 84.
- [17] S.W. Tao, J.T.S. Irvine, *Nat. Mater.* 2 (2003) 320.
- [18] R.M. Xing, Y.R. Wang, S.H. Liu, C. Jin, *J. Power Sources* 208 (2012) 276.
- [19] S. Zha, P. Tsang, Z. Cheng, M. Liu, *J. Solid State Chem.* 178 (2005) 1844.
- [20] S.W. Tao, J.T.S. Irvine, J.A. Kilner, *Adv. Mater.* 17 (2005) 1734.
- [21] S.W. Tao, J.T.S. Irvine, S.M. Plint, *J. Phys. Chem.* 110 (2006) 21771.
- [22] D.M. Bastidas, S.W. Tao, J.T.S. Irvine, *J. Mater. Chem.* 16 (2006) 1603.
- [23] S.P. Jiang, L. Zhang, Y.J. Zhang, *J. Mater. Chem.* 17 (2007) 2627.
- [24] S.B. Ha, P.S. Cho, Y.H. Cho, D. Lee, J.H. Lee, *J. Power Sources* 195 (2010) 124.
- [25] V.V. Kharton, E.V. Tsipis, I.P. Marozau, A.P. Viskup, J.R. Frade, J.T.S. Irvine, *Solid State Ionics* 178 (2007) 102.
- [26] X. Zhang, M. Robertson, C. Deces-Petit, W. Qu, O. Kesler, R. Maric, D. Ghosh, *J. Power Sources* 164 (2007) 668.
- [27] C.O. Park, S.A. Albar, W. Weppner, *J. Mater. Sci.* 38 (2003) 4639.
- [28] Y.X. Shi, C. Li, N.S. Cai, *J. Power Sources* 196 (2011) 5526.
- [29] Y.X. Li, J. Zhou, D.H. Dong, Y. Wang, J.Z. Jiang, H.F. Xiang, K. Xie, *Phys. Chem. Chem. Phys.* 14 (2012) 15547.
- [30] S.W. Tao, J.T.S. Irvine, *Chem. Mater.* 18 (2006) 5453.
- [31] S.W. Tao, J.T.S. Irvine, *J. Electrochem. Soc.* 151 (2004) A252.